Collagenous Skeleton of the Rat Mystacial Pad

SEBASTIAN HAIDARLIU,[1]* EREZ SIMONY,[1] DAVID GOLOMB,[2] AND EHUD AHISSAR[1]

[1]Department of Neurobiology, The Weizmann Institute of Science, Rehovot, Israel
[2]Department of Physiology and Zlotowski Center for Neuroscience, Ben-Gurion University of the Negev, Beer-Sheva, Israel

ABSTRACT

Anatomical and functional integrity of the rat mystacial pad (MP) is dependent on the intrinsic organization of its extracellular matrix. By using collagen autofluorescence, in the rat MP, we revealed a collagenous skeleton that interconnects whisker follicles, corium, and deep collagen layers. We suggest that this skeleton supports MP tissues, mediates force transmission from muscles to whiskers, facilitates whisker retraction after protraction, and limits MP extensibility. Anat Rec, 294:764–773, 2011. © 2011 Wiley-Liss, Inc.

Key words: rat mystacial pad; autofluorescence; collagenous skeleton; momentum transmission; collagenase

In studies of active tactile sensing, the motor plant of the rodent mystacial pad (MP) has been used to study coordinated and precise whisker movements (Hill et al., 2008; Knutsen et al., 2008; Grant et al., 2009; Simony et al., 2010). The orderliness of simultaneous vibrissal movements during whisking spurred our search for a mechanism that enables highly coordinated movements of the vibrissae, which may be similar to those previously described for cardiac and lung skeletons that consist of fibrous collagen frameworks (Caulfield and Borg, 1979; Cavalcante et al., 2005; Pope et al., 2008). In the mouse MP, connective tissue fibers in bands parallel to the skin surface connect, in a plate-like fashion, the lower parts of two neighboring follicles in the same row (Dörfl, 1982). In contrast, in the hamster MP, there is a loosely organized layer of connective tissue fibers in the immediate subcapsular zone (Wineski, 1985). Involvement of connective tissue in tying the capsule to the hair follicle has been described in rats (Vincent, 1913). Despite the obvious importance of collagen for the mechanical properties of the MP, until now little has been revealed about the structural organization of collagen in the entire MP.

In whisking rodents, MPs are specifically organized and contain four basic tissue types. Starting from the outside, the first is the corium, which is covered by epithelial tissue that rests on a layer of connective tissue. Within the last, follicle-sinus complexes (FSCs) and elements of nervous and muscular tissue are present. According to Dörfl (1982), the proximal ends of FSCs are interconnected by a fibrous plate. Furthermore, the subcapsular zone of hamsters contains rostrocaudally oriented connective tissue fibers (Wineski, 1985). As rodent whiskers have no direct contact with the muscles, the aim of this study was to clarify the role of the extracellular matrix (ECM) in transmission of momentum from MP muscles to MP whiskers.

Collagen, which is produced by fibroblasts, is thought to determine the mechanical properties of the MP. Densely packed collagen fibers provide both strength and resistance to tearing and stretching (Caulfield and Borg, 1979). Intrinsic collagenous and non-collagenous fluorophors of the skin and muscles can be directly visualized by various fluorescence microscopy methods

Grant sponsor: European Commission; Grant number: BIOTACT (ICT-215910); Grant sponsors: The Minerva Foundation funded by the Federal German Ministry for Education and Research; United States—Israel Binational Science Foundation; Grant number: 2007121.

*Correspondence to: Sebastian Haidarliu, Department of Neurobiology, The Weizmann Institute of Science, Rehovot 76100, Israel. Fax: +972-8-9346099. E-mail: sebastian.haidarliu@weizmann.ac.il

Received 29 September 2010; Accepted 26 January 2011

DOI 10.1002/ar.21371

Published online 17 March 2011 in Wiley Online Library (wileyonlinelibrary.com).

(Skala et al., 2005). Autofluorescence (AF) of collagen occurs due to crosslinks, including non-enzyme-dependent ones, between collagen fibers. AF of the MP muscles is caused by the presence of collagen in the epi-, peri-, and endomysium, and of other fluorophores, such as nicotinamid and flavin adenine dinucleotides, proteins, and pigments (Andersen and Wold, 2003). After tissue staining for cytochrome oxidase (CCO), the AF of free collagen fibers in the MP was not changed, whereas that of muscles due to the presence of collagen and other muscle fluorophors was no longer detectable (Haidarlui, unpublished data). The histochemical reaction for demonstration of CCO activity is based upon oxidative polymerization of diaminobenzidine (DAB), and reflects mitochondrial CCO activity (Seligman et al., 1968; Reith and Schuler, 1972). However, conversion of the DAB into a dark homogenously distributed, non-fluorescent product quenches the fluorescence that was induced within the neurons by different fluorescent markers (Lübke, 1993). Similar quenching of co-localized fluorescence caused by diffuse DAB staining of cell nuclei was also reported (Yamada et al., 2005). In muscles, mitochondria are distributed within different pools, such as, subsarcolemmal, perivascular, intersarcomeric, and paranuclear (Rothstein et al., 2005), so local absorption of exciting or emitted light by diffuse DAB polymerization products may extinguish muscle AF.

Here, we present evidence that supports the presence of a collagenous skeleton in the rat MP, a skeleton that we assume determines the anatomical and functional integrity of the entire MP. The organization of the collagen within the rat MP was revealed by collagen AF after excitation with UV light in histological slices stained for CCO. Histological samples were obtained from young and adult male albino Wistar rats and processed as previously described (Haidarliu et al., 2010). Briefly, MPs were sectioned into 60 μm thick slices in coronal, tangential (parasagittal), and horizontal planes. The slices were fixed with paraformaldehyde, stained for CCO, and coverslipped with Krystalon (Harleco; Lawrence, KS). Structures containing CCO and collagen were visualized by light and fluorescence microscopy, respectively, using a Nikon Eclipse 50i fluorescent microscope. Excitation of AF was attained at 350–370 nm using a standard Nikon excitation filter CY3, which causes emission of blue AF at ~440 nm (Odetti et al., 1992; Kollias et al., 1998; Na et al., 2001). These wavelengths are a reliable fluorescent biomarker for collagen (Georgakoudi et al., 2002). Confirmation that collagen was the source of AF was achieved by incubating portions of unstained and CCO-stained tissue slices with *Clostridiopeptidase* A, EC 3.4.24.3 (0.5 mg/mL in 0.05 M Tris buffer, pH 7.6, containing 0.001 M $CaCl_2$) at room temperature, which produces a collagenolytic effect (Johanson and Pierce, 1972).

RESULTS

In unstained tangential slices of the rat MP (Fig. 1A), muscle fibers possessed a blue AF (Fig. 1B). Both extrinsic and intrinsic muscle AF was extensive, and interfered with visualization of collagen fibers by AF (Fig. 1C,D). Staining for CCO activity permitted visualization of tissue morphology by bright-field microscopy (Fig. 1E), while extinguishing the AF of collagen and other minor fluorophors in extrinsic and intrinsic muscles (Fig. 1F–H).

The general architecture of the MP and its collagenous structures was visualized in coronal slices of the snout of young rats by staining for CCO (Fig. 2A) and viewing the distribution of blue AF (Fig. 2B). The borders of the slices were easily determined by the bright AF of the superficial layers of the corium. The fluorescence of the distal ends of the capsules continued into the corium. In fact, at high magnification of slices obtained by cutting the corium at an angle of ~45° to the surface of the MP (Fig. 3A,B), collagen fibers of the distal end of the capsule continued into the superficial mesh.

In transversal slices of the FSCs of adult rats, a spongy three-dimensional network composed of thin collagen fibers filled the lower part of the cavernous sinus (CS) (Fig. 4A). In the distal area of the CS, thick collagenous trabeculae, reported as early as 1913 (Vincent, 1913), were clearly seen in longitudinally cut FSCs (Fig. 4B). The space between the inner surface of the capsule and mesenchymal sheath was filled by a collagen network and trabeculae. The lengths of the capsules appeared to determine the distance between the corium and plate, because their shape was not affected by different manipulations (folding, stretching, and flattening) during histological treatment. This supports the use of the term "rigid bodies" for FSCs in a model of the biomechanical plant of the rat MP (Simony et al., 2010), although it may refer mainly to the capsules of the FSCs, and only partially to their hair shafts.

The proximal ends of the follicle capsules come into contact with a collagen layer that was called the "plate" by Dörfl (1982). In rats, we observed that this plate consists of a spongy network of thin interlacing collagen fibers that form a continuous soft layer that encases the proximal ends of vibrissal follicles. In this collagen layer, which is between proximal ends of FSCs, large areas were more organized, and could be considered as a quasi-hexagonal mesh (Fig. 5). The fibers of this collagen layer, due to splitting and joining, formed hexagons of 30–40 μm in diameter, similar to the mesh of fibers previously described in muscle and adipose tissues of the heart (Caulfield and Borg, 1979; Swatland, 1987; Pope et al., 2008), and in lung (Cavalcante et al., 2005). This layer of the collagenous skeleton may correspond to the hypodermis of the skin that consists of adipose tissue. In mice, Dörfl (1982) revealed that follicles with their muscle slings are located in adipose tissue. In the MP of the rat, we observed only a thin (~0.5 mm thick) layer of adipose tissue. More superficially, at the level of blood sinuses and the extremities of the intrinsic muscles, adipose tissue was absent (Fig. 6). The quasi-hexagonal collagenous mesh was attached to the proximal ends of the FSCs. It contained adipocytes filled with droplets of uncompressible fat and surrounded by the woven collagen network that resembles closed cell foam. These characteristics might allow the layer to serve both as a supporting framework for the follicles, as well as a resilience system that provides a uniform distribution of the stresses and strains due to whisking.

Under the layer formed by the quasi-hexagonal deep mesh, we revealed a subcapsular fibrous mat that consisted of thick fibers of collagen, which was similar to the subcapsular layer described by Wineski (1985). The fibers of this layer touched the proximal ends of the

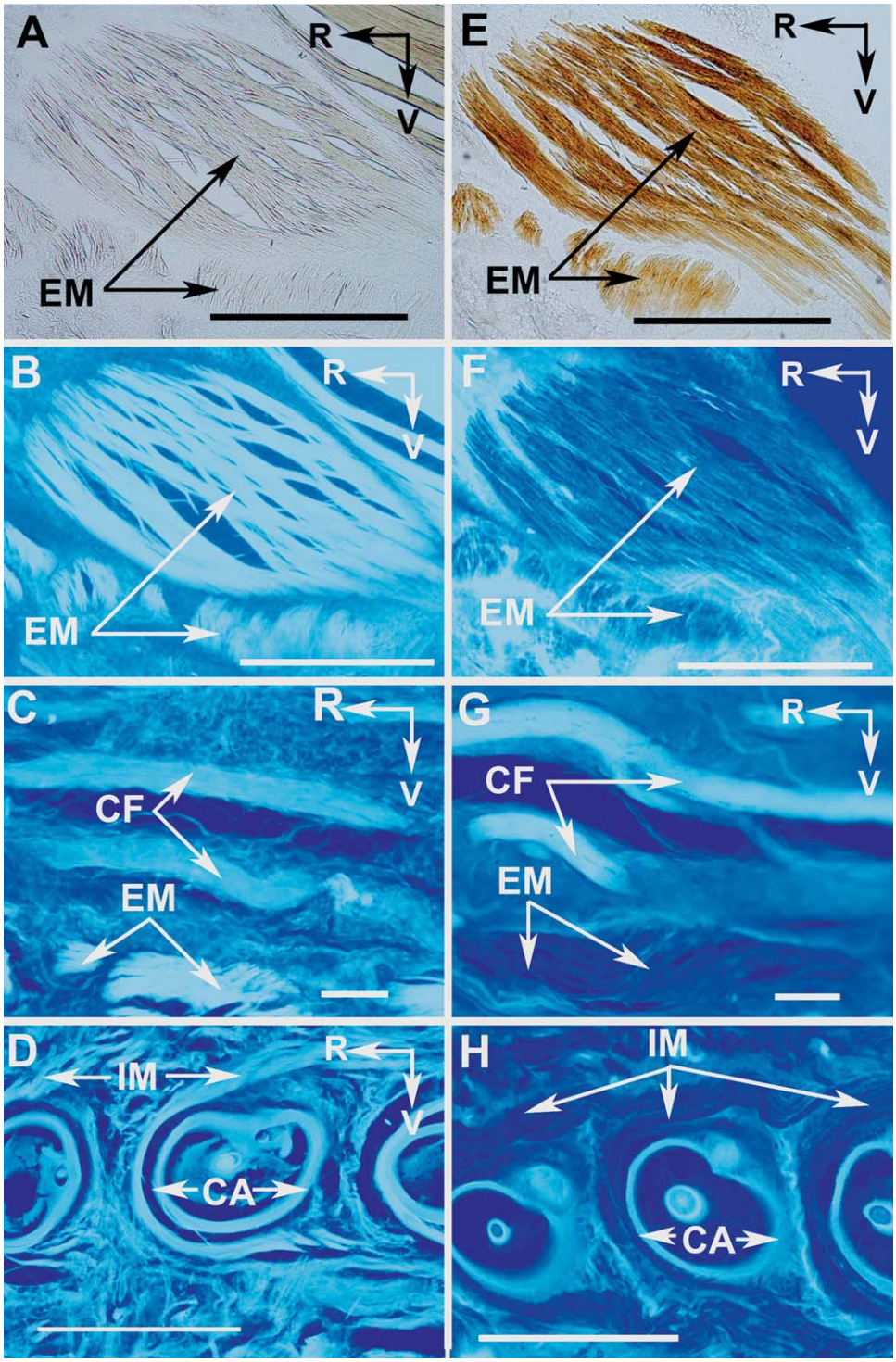

Fig. 1. Effect of staining for CCO on collagen AF in tangential slices of the rat MP. Bright-field images of unstained (**A**) and stained for CCO (**E**) slices. Collagen and muscle AF in unstained (**B–D**) and stained for CCO slices (**F–H**). CA, capsule; CF, collagen fibers of the subcapsular fibrous mat; EM, extrinsic muscles; IM, intrinsic muscles; R, rostral; V, ventral. Scale bars = 0.1 mm in panels C and G, and 1 mm in the others.

vibrissal follicles, and consisted mainly of long thick wavy fibrous fascicles of collagen, with a wide range of sizes, that were oriented rostro-caudal (Figs. 2 and 7). This layer was represented mostly by a single row of collagen fibers, the extensions of which could also be observed in the deep mesh (Fig. 5). However, in the central area of the maxillary part of the fibrous mat, under the FSCs that are represented in the thalamus by the

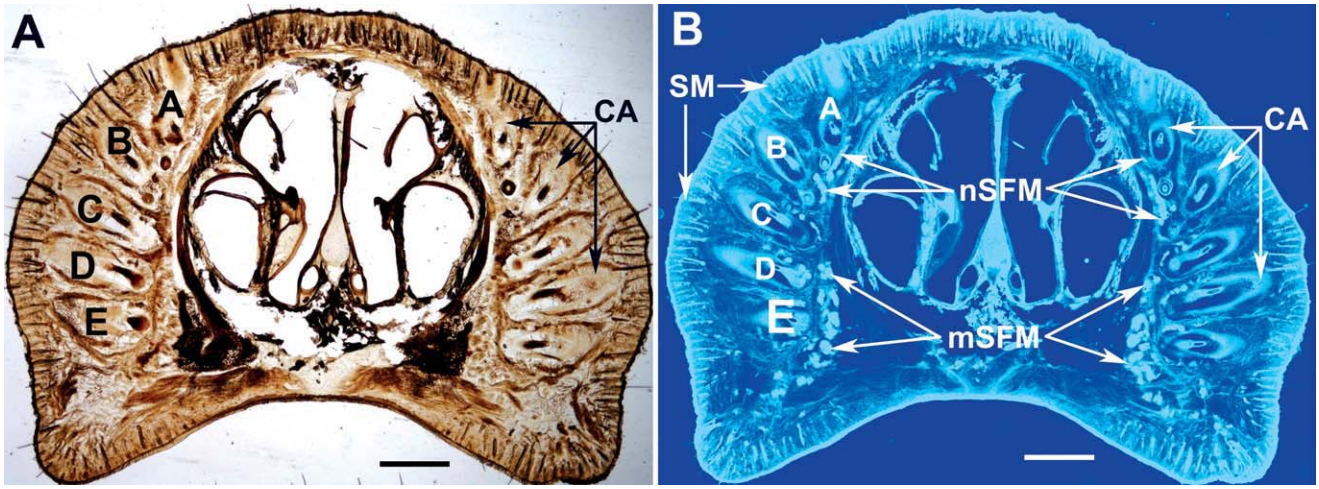

Fig. 2. Light microscopy (**A**) and AF (**B**) of a coronal slice stained for CCO of the snout of a young rat. A–E, FSCs that form an arc; CA, capsules; mSFM and nSFM, maxillary and nasal parts of the subcapsular fibrous mat, respectively; SM, superficial mesh. Scale bars = 1 mm.

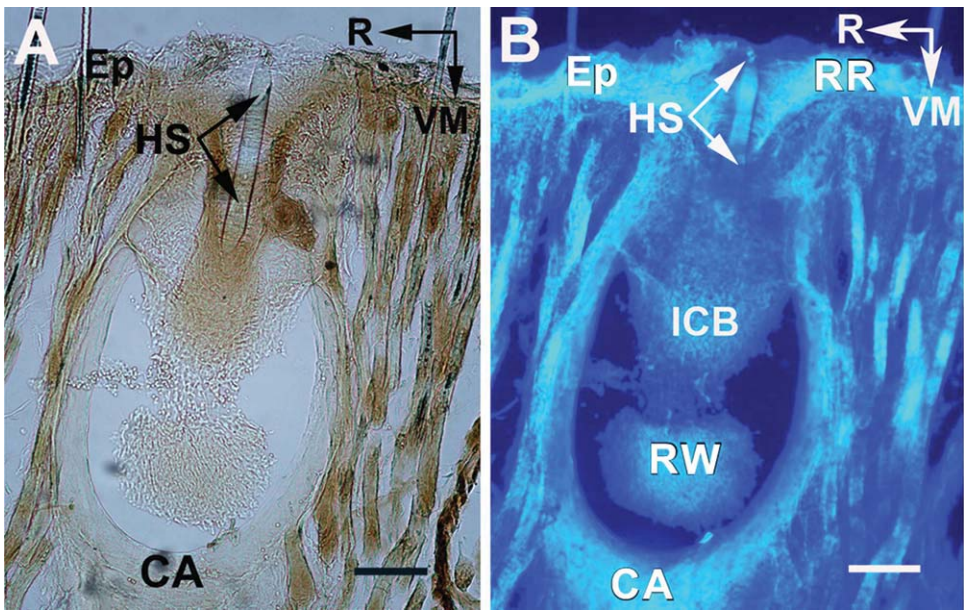

Fig. 3. The "mouth" of a FSC in an oblique superficial slice. Light microscopy (**A**) and AF (**B**) views. CA, vibrissal capsule; Ep, epidermis; HS, hair shaft; ICB, inner conical body; R, rostral; RR, rete ridge collar; RW, ringwulst; VM, ventromedial. Scale bars = 0.2 mm.

largest barreloids (Haidarliu and Ahissar, 2001), two to three rows of thick collagen fibers were observed (Figs. 2 and 8). More caudal, after passing the level of straddlers, collagen fibers of both nasal and maxillary parts of the MP converged and anchored to the maxilla.

The mechanical role of the collagen fibers of the quasi-hexagonal deep mesh and the subcapsular fibrous mat (the two layers described above) might consist of returning the proximal ends of the FSCs to their initial (resting) position after being displaced during a whisker protraction caused by muscle contraction. Furthermore, these collagen fibers might be essential for maintaining a constant position of the proximal ends of whisker follicles relative to each other.

Incubation with *Clostridium* collagenase of slices that contain the subcapsular fibrous mat revealed a progressive reduction of the intensity of blue AF, which confirms that collagen is a major component of the MP skeleton. Exposure to the collagenase caused the AF of the thin fibers to disappear completely, and although the thicker

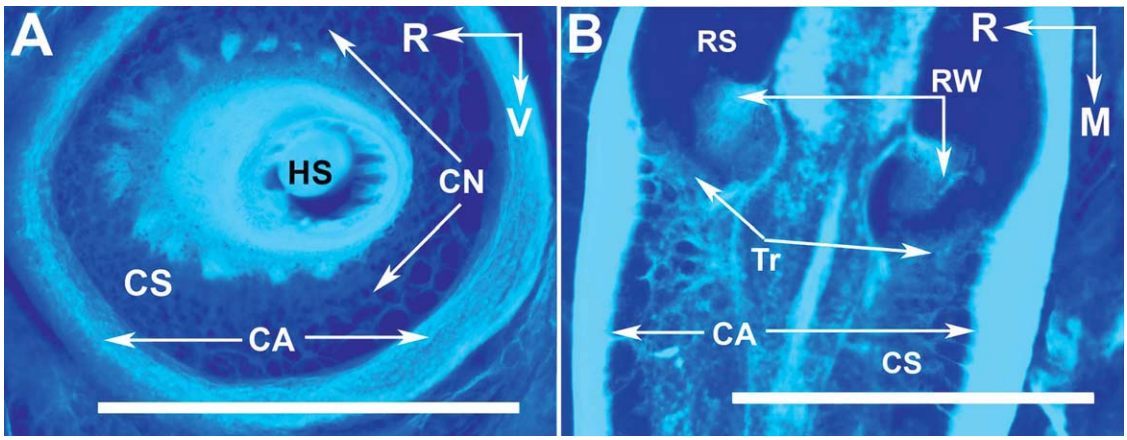

Fig. 4. Autofluorescence of the collagenous network (CN) and trabeculae (Tr) in transversally (**A**) and longitudinally (**B**) cut FSCs. CA, capsule; CS, cavernous sinus; HS, hair shaft; M, medial; R, rostral; RS, ring sinus; RW, ringwulst; V, ventral. Scale bars = 1 mm.

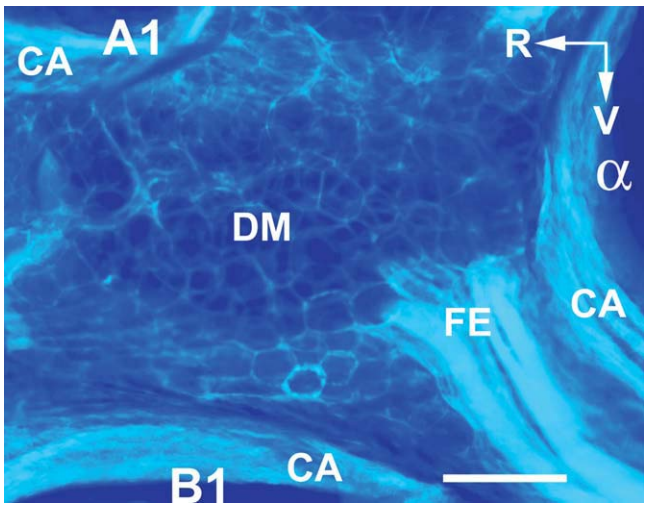

Fig. 5. Collagen AF in a tangential slice of an adult rat MP at the level of the deep mesh (DM) that is attached to the capsules (CA) of the vibrissae A1 and B1, and of the straddler α. FE, fiber extension of the subcapsular fibrous mat; R, rostral; V, ventral. Scale bar = 0.1 mm.

fibers were still visible, their diameter diminished (Fig. 9). After 90 min of exposure, cloudy material accumulated around thick collagen fibers.

DISCUSSION

Our findings support the collagenous skeleton of the MP being involved in maintaining follicle and whisker alignment, as well as MP shape and size. The collagen of the MP skeleton is intimately associated with intrinsic and extrinsic muscles, and with FSCs. This collagenous skeleton appears to be the principal force-bearing structure of the rat MP. Although not a bony ("true") skeleton, it can provide structural support and function for

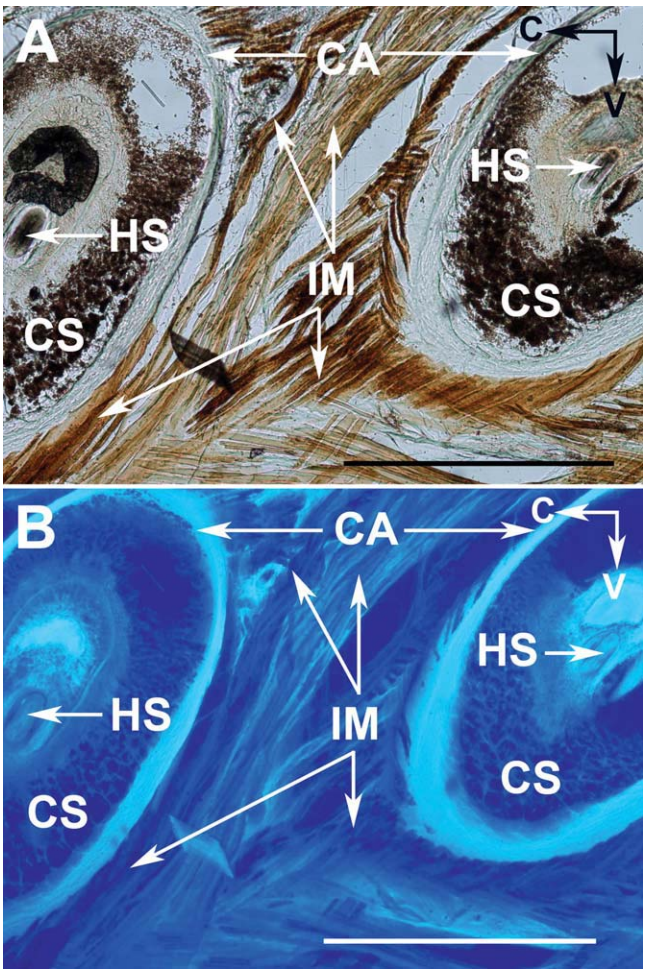

Fig. 6. Light microscopy (**A**) and AF (**B**) of a tangential slice of an adult rat MP at the level of cavernous sinus (CS). C, caudal; CA, capsule; HS, hair shaft; IM, intrinsic muscle; V, ventral. Scale bars = 1 mm.

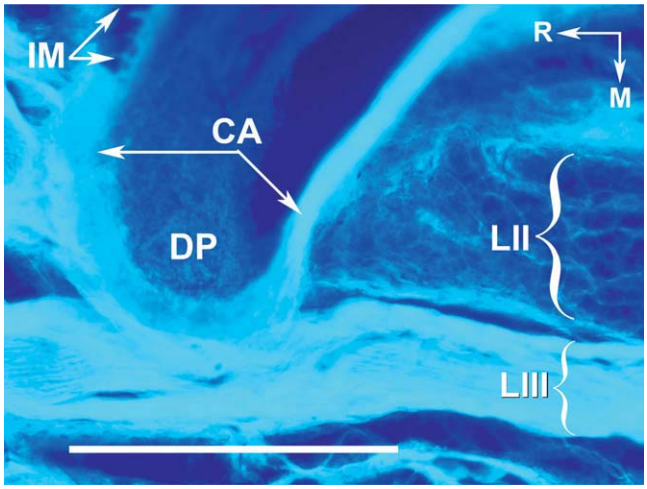

Fig. 7. Collagen AF in the deep mesh (LII) and in subcapsular fibrous mat (LIII) in a horizontal slice of an adult rat MP. CA, capsule; DP, dermal papilla; IM, intrinsic muscle; M, medial; R, rostral. Scale bar = 1 mm.

the MP. Within the core of the MP, the collagen skeleton may maintain spatial orientation of FSCs during whisking. When tractive forces produced by the extrinsic muscles are applied to the superficial and deep layers of the collagenous skeleton, they are probably transmitted through linkage "joints" to the proximal and distal ends of the FSC capsules. As the whiskers have no direct contact with the muscles, their active movements are completely controlled by the movements of the FSCs. Within the FSCs, delicate fibers, continuous with the fibers of the capsule, extend across the CS and adhere to the glassy membrane that separates the mesenchymal sheath of the hair follicle from external root sheath (Melaragno and Montagna, 1953).

The skeleton of the MP involves one superficial and two deep (quasi-hexagonal mesh and subcapsular fibrous mat) collagen layers, which are connected to each other by the capsules of the FSCs (Table 1). According to the classification proposed by Ottani et al. (2001), the subcapsular fibrous mat may be composed of fibrils that belong to the T-type form, and the quasi-hexagonal mesh may contain fibrils of the C-type. The T-type fibrils are arranged in large and heterogenous bundles oriented parallel to tensile stress along their axes, and are not extendable. During protraction, they straighten, and during retraction, they restore their initial wavy shape. The C-type fibrils are small and homogenous. They resist to multidirectional stresses, forming sheets with a quasi-hexagonal mesh. Similar organization of a meshwork of branched, small diameter fibers composed of Type III collagen was described in adipose tissue of the pig (Swatland, 1987). In aquatic animals, such as harbor seals, high mobility of vibrissa can be facilitated by unsaturated fatty acids with low melting points that are present in adipose tissue near the vibrissa (Dehnhardt et al., 1998). In the mouse MP, the plate-like layer appears like a "fenestrated ribbon" (Dörfl, 1982). This can now be explained as a representation of the adipose tissue maintained by a collagenous quasi-hexagonal network, the fibers of which are attached to the proximal ends of FSCs.

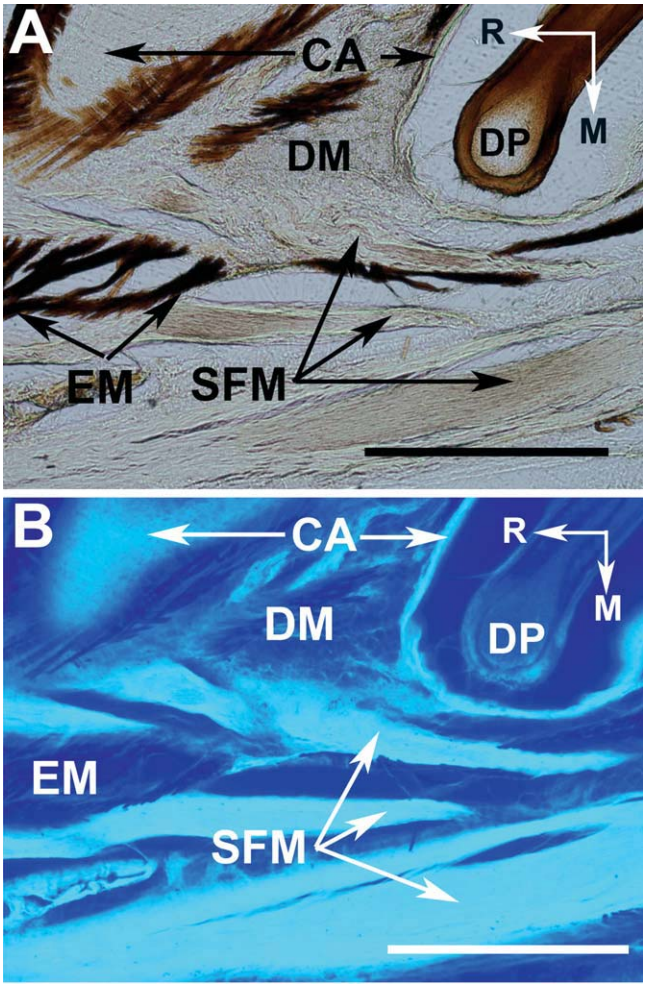

Fig. 8. Light microscopy (**A**) and AF (**B**) of a horizontal slice of an adult rat MP. CA, capsule; DM, deep mesh; DP, dermal papilla; EM, extrinsic muscle; M, medial; R, rostral; SFM, subcapsular fibrous mat. Scale bars = 1 mm.

Our findings support the previously reported tight relationship between hair follicles and adipose tissue in rats (Hausman et al., 1981). During development of the rat hypodermis, adipocytes are observed only around the lower part of the hair follicles, where they form a layer in direct contact with cells of the external root sheath. Cultured dermal papilla of the adult rat vibrissal follicle is also capable of spontaneous adipogenic differentiation (Jahoda et al., 2003).

In the rat mystacial pad, adipocytes and ECM are constantly subjected to spatial deformations caused by whisking. Though the impact of mechanical forces on the differentiation and morphology of the ECM has not yet been studied in depth, certain mechanisms that prevent tissue disruption by mechanical forces have been described (Mariman and Wang, 2010). In the rat MP, we observed some features that were characteristic for the adipose tissue of the deep mesh.

i. Layer II of the collagenous skeleton was thin (~0.5 mm) and contained adipocytes encased in a quasi-hexagonal mesh. This mesh was reinforced

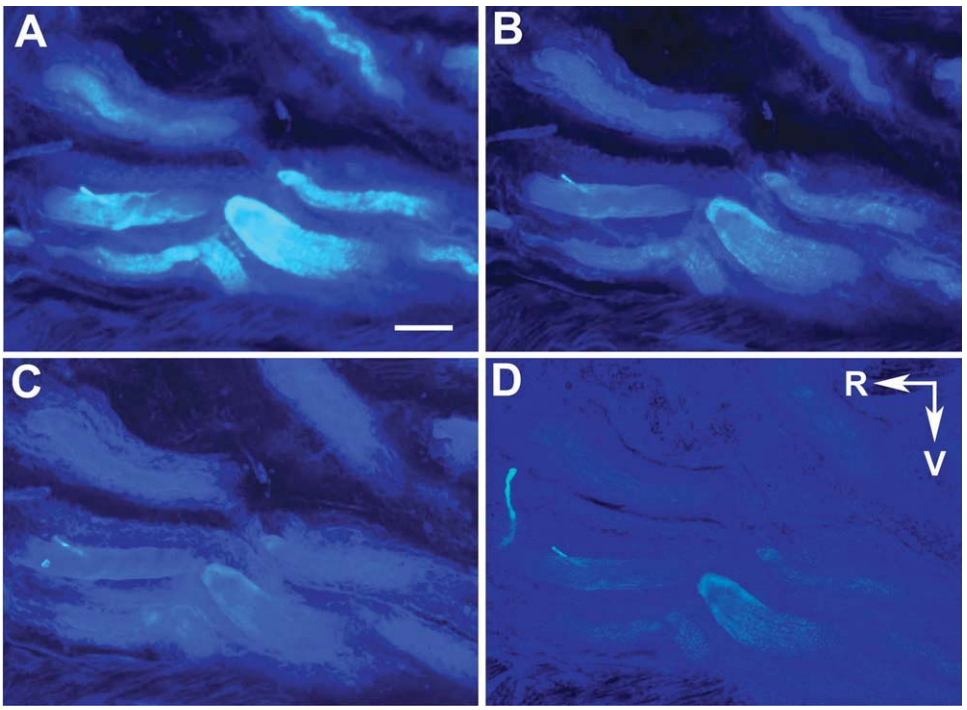

Fig. 9. Collagen AF of the subcapsular fibrous mat before (**A**) and after incubation with *Clostridiopeptidase* A for 30 min (**B**), 60 min (**C**), and 90 min (**D**). R, rostral; V, ventral. Scale bar = 0.2 mm.

by collagen fibers, similar to hypodermal adipose tissue (Motta, 1975; Comley and Fleck, 2010). Some of these collagen fibers originated from the subcapsular fibrous mat (Fig. 5).

ii. In Layer II, the adipocytes were ~40 μm in diameter. The diameters of adipocytes in other regions of the rat body were reported to be 50–80 μm (Askew and Hecker, 1976; Jamdar et al., 1981, 1986) whereas those of pigs and humans were reported to be 70 μm and 30 to 70 μm, respectively, (Geerlings et al., 2008).

iii. In the deep mesh, ECM was continuous and connected neighboring FSCs (Fig. 5). Collagen fibers of the ECM were attached to the lower capsular part of the FSCs.

iv. In the microtome slices of the rat MP, the surface of contacts between the neighboring adipocytes was flat which means that the shape of the adipocytes should be polyhedronic. In the other regions of the rat body, adipocytes are reportedly mostly spherical (Avram et al., 2005).

In light of the above, we conclude that Layer II of the rat MP can be considered to be a layer of adipose tissue in which adipocytes are encased in a strong collagenous mesh. This mesh is a part of the collagenous skeleton, is attached to vibrissal capsules and can function as springs and dampers simultaneously. Non-compressible fat droplets within the collagenous polyhedra facilitate the resilience of this layer during whisking.

In the core of the MP, the collagenous skeleton consists of strong rigid capsules of the FSCs. These capsules are comprised of thick collagen fibers that form a strong wall (Sakita et al., 1994), and can accomplish their function when the sinuses are filled with blood. The sinuses are supplied with blood directly from the branches of the arterioles. High blood pressure within the capsule increases turgidity, which is necessary to stabilize mechanical properties of the vibrissa during sensory exploration (Rice, 1993). The distal ends of the capsules continue into the collagen mesh of the corium, and their proximal ends are attached to the collagen fibers of the two deep collagen layers (see above) to form a connection that can function as a semi-ball joint. Such connections enable the whisker shaft to move in all directions within a plane that is parallel to the whisker pad surface.

Attachments of the distal and proximal ends of the FSCs to the relevant collagenous layers create conditions favorable for synchronous vibrissal movements by facilitating side-to-side coupling and by minimizing the possibility of transverse vibrissa deviations during whisking. The wavy, coarse collagen bundles of the subcapsular fibrous mat are crucial viscoelastic structures of the skeleton, which retract whiskers after their protraction. These collagen fibers were oriented in parallel, and along the direction of the largest tension generation, similar to those of the fibrous heart skeleton (see Icardo and Colvee, 1998), and were attached, rostral, to the rostrolateral pole of the premaxilla and nasal cartilage, and caudal, to the maxilla.

One unexpected function of the MP skeleton is to facilitate movements, but in opposite directions, of the corium and deep collagen layers, the planes of which are parallel. This is possible because the stiff capsules of the FSCs cannot be compressed or extended during muscle contraction. In fact, the distance between the deep

TABLE 1. Collagenous layers of the rat MP

	Layer I	Layer II	Layer III
Layer name	Superficial mesh	Deep mesh	Subcapsular fibrous mat
Location	Immediate subepidermal corium	Around proximal ends of the FSCs	Medial to the proximal ends of the FSCs
Semblance	Continuous interlacing flexible plexus	Fenestrated plate[a] composed of polygons that contain adipocytes	Loose long wavy fibers[b,c] along the rows of FSCs
Structure size	Fiber diameters of 20–30 μm	Fiber diameters of 5–15 μm, polygons (adipocytes) of ~40 μm in diameter[d,e,f]	Fiber diameters of 100–300 μm; lengths of 3–4 mm or more
Collagen type	Mainly Type I[g,h]	Co-polymers of types I, III, V; C-type fibrils[i]	Mainly Type I fibrous collagen; T-type fibrils[i]
Mechanical properties	Multidirectional extension and backlash	Multidirectional extension and backlash	Unidirectional resilience of wavy fibers
Fiber orientation	At random, mainly parallel to the skin[j]	Multidirectional, forming quasi-hexagons in the plane parallel to the skin	Rostro-caudal, parallel to each other in parasagittal plane
Anchoring	To the distal capsular ends and skin collagen layer, along the perimeter of the MP	To the proximal capsular ends, and to subcapsular fibrous mat by the aid of fiber extensions	Caudal, to maxilla; rostral, to rostro-lateral pole of the premaxilla and nasal cartilage

[a]Dörfl, 1982.
[b]Wineski, 1985.
[c]Ushiki, 2002.
[d]Askew and Hecker, 1976.
[e,f]Jamdar et al., 1981, 1986.
[g]Lanir, 1979.
[h]Birk and Bruckner, 2005.
[i]Ottani et al., 2001.
[j]Kawamata et al., 2003.

collagen layers and corium increases during protraction, and is maximal when the long axes of FSCs form a rectangle with the deep collagen layers and corium. The collagenous skeleton of the rat MP also limits the extension of the MP tissues. Moreover, the skeleton is a dynamically active entity. The MP skeleton retracts whiskers after protraction caused by muscle contraction, prevents exceeding torsional deformation (Knutsen et al., 2008), and controls movement of the corium in relation to the deep collagen layers of the MP.

On the basis of what is now known about the network of the MP collagenous skeleton, we propose a new schematic bio-mechanical model of the rat MP (Fig. 10). This new 3D model includes three connective tissue layers, whereas a reduced 2D model we previously proposed (Haidarliu et al., 2010) only included two such layers. The first layer (Superficial mesh) consists of a subepidermal layer of connective tissue fibers that are arranged at random and form an interlacing plexus (Fig. 10, Layer I). It is a 2D layer in which forces can be applied along both the rostrocaudal (RC) and dorsoventral (DV) axes. This layer can be pulled caudal by the *M. nasolabialis* and *M. maxillolabialis* (corium whisker retractor, CR) to cause whisker retraction, and rostral, by the Pars media superior and inferior of the *M. nasolabialis profundus* (corium whisker protractor, CP) to cause whisker protraction. The second layer (Deep mesh), which consists of a fenestrated plate composed of a collagenous mesh with encased adipocytes (Figs. 5 and 10, Layer II), is also a 2D layer in which forces can be applied along both the RC and DV axes. The third layer (Subcapsular fibrous mat) consists of parallel collagen fibers anchored rostral to the premaxilla and nasal cartilage, and caudal to the rostral part of the maxilla (Fig. 10, Layer III). It is a 2D layer in which forces can only be applied in the RC direction. Layer III can be pulled rostral by the mat whisker retractor (MR), which is comprised of the three parts of the *M. nasolabialis profundus* that cause whisker retraction (Haidarliu et al., 2010). This is possible because, in the whisker resting position, the fibers of this layer are undulated, and can be straighten by muscle contraction. Layers I and II act locally during deformation of the surrounding tissues (at anchor points between follicles) whereas Layer III effectively connects all the bases of FSCs in a row, similar to the suggestion of Hill et al. (2008). Even though their bases are connected, removing one FSC from a vibrissal row should not affect the integrity of the collagenous layers of the MP.

The skeleton of the MP includes the origins and insertion sites for the MP muscles. The intrinsic muscles of the MP are attached to the capsules of two neighboring FSCs in a row, and to the corium. The extrinsic muscles of the MP originate from various sites on the facial skull bones or from the nasal cartilage. Their insertion (anchor) sites are in the corium or the subcapsular fibrous mat. In the corium, most of these insertion sites are specifically organized to form spreads of tapered fibers reminiscent of rosettes. Such spreading of insertion sites facilitates synchronous movements with uniform trajectories for all of an individual's vibrissae during whisking. The skeleton receives external loads from the extrinsic muscles, and transfers the impelling momentum to the whiskers.

Incubation with *Clostridium* collagenase (Clostridiopeptidase A) of MP slices containing fibers of the subcapsular fibrous mat caused a decrease in AF of collagen fibers. A similar progressive degradation of collagen was

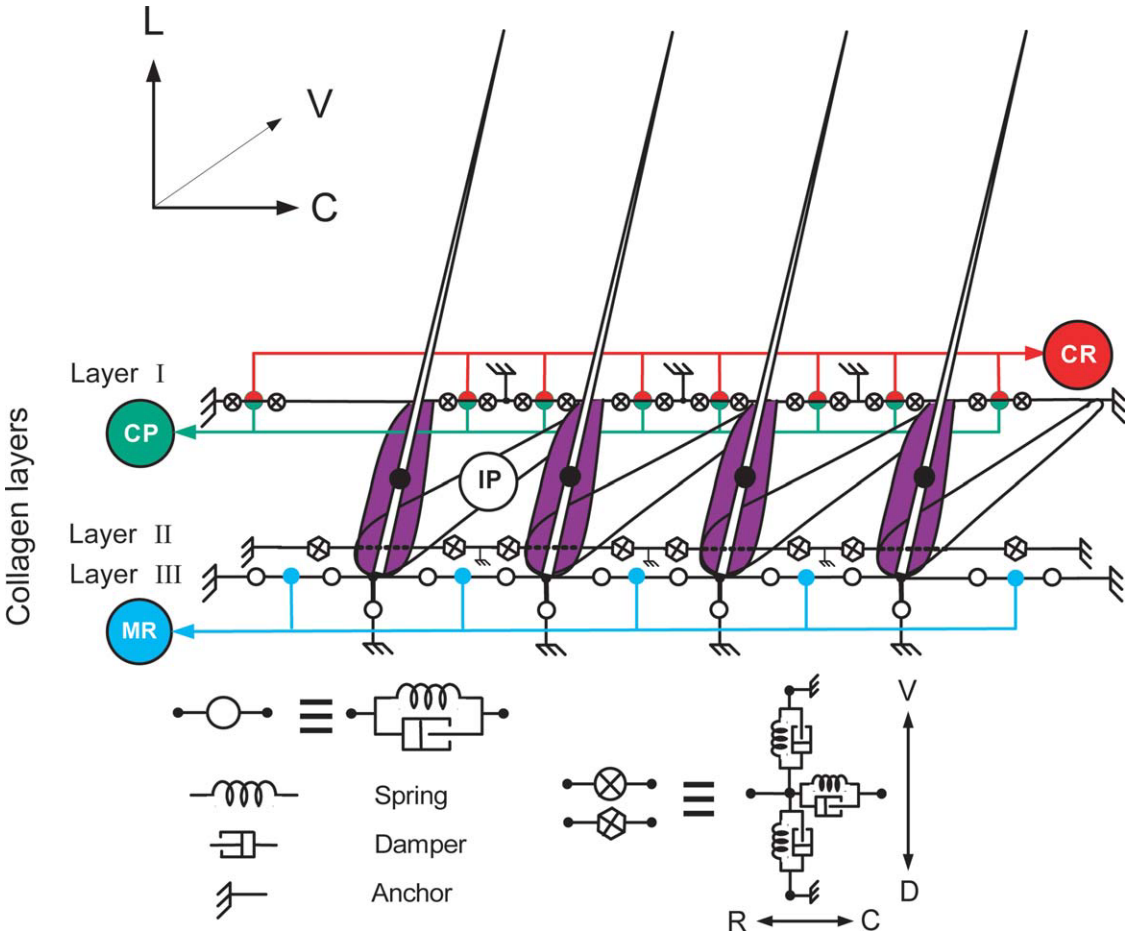

Fig. 10. Schematic drawing of a three-dimensional biomechanical model that represents one vibrissal row of the rat MP in resting position. Layer I, Superficial mesh; Layer II, Deep mesh; Layer III, Subcapsular fibrous mat; CP, corium whisker protractor (green lines and semicircles in Layer I); CR, corium whisker retractor (red lines and semicircles in Layer I); IP, intrinsic whisker protractor (oblique lines that connect neighboring FSCs); MR, mat whisker retractor (blue lines and circles in Layer III). Solid black circles represent the vibrissal centers of mass. Empty circles represent springs coupled with dampers, which symbolize the elasticity of the tissue along the rostrocaudal (RC) axis. Crossed circles and hexagons represent springs coupled with dampers along the RC and DV axes in Layers I and II, respectively. Anchors represent non-elastic sites in the MP. Dashed lines in Layer II indicate that this layer surrounds the FSCs. C, caudal; L, lateral; D, dorsal; V, ventral.

observed in liver slices upon incubation with bacterial collagenase (Perez-Tamayo and Montfort, 1980). During application of *Clostridium* collagenase to structurally intact collagen fibers of the rat tail, the diameter of the fibers decreases continuously, which indicates a degradation process (Wyatt et al., 2009). *Clostridium* collagenase does not digest some types of collagen, such as Type VI collagen, a microfibrillar collagen that assembles into hexagonal-like networks (Wiberg et al., 2002; Shi et al., 2010). This might explain why large collagenous fibers, though diminished in diameter, were still seen when we exposed the subcapsular fibrous mat to *Clostridium* collagenase.

In summary, in the rat MP, we revealed a fibrous collagenous skeleton by fluorescent microscopy of intrinsic MP fluorophores. This skeleton consists of superficial and deep collagen layers interconnected by collagenous capsules of the FSCs. It is an integrated framework that satisfies the functional requirements of whisking behavior. We suggest that the fibrous collagenous skeleton of the MP is able to support the tissues of the MP, to transform muscle-impelling momentum into whisker movements, to facilitate passive whisker retraction, and to control the extension of MP tissue.

ACKNOWLEDGMENTS

Ehud Ahissar holds the Helen Diller Family Professorial Chair of Neurobiology. The authors thank Dr. Barbara Schick for reviewing the manuscript.

LITERATURE CITED

Andersen CM, Wold JP. 2003. Fluorescence of muscle and connective tissue from cod and salmon. J Agric Food Chem 51:470–476.

Askew EW, Hecker AL. 1976. Adipose tissue cell size and lipolysis in the rat: response to exercise intensity and food restriction. J Nutr 106:1351–1360.

Avram AS, Avram MM, James WD. 2005. Subcutaneous fat in normal and diseased states. 2. Anatomy and physiology of white and brown adipose tissue. J Am Acad Dermatol 53:671–683.

Birk DE, Bruckner P. 2005. Collagen suprastructures. Top Curr Chem 247:185–205.

Caulfield JB, Borg TK. 1979. The collagen network of the heart. Lab Invest 40:364–372.

Cavalcante FCA, Ito S, Brewer K, Sakai H, Alencar AM, Almeida MP, Andrade JS, Majumdar A, Ingenito EP, Suki B. 2005. Mechanical interactions between collagen and proteoglycans: implications for the stability of lung tissue. J Appl Physiol 98: 672–679.

Comley K, Fleck NA. 2010. A micromechanical model for the Young's modulus of adipose tissue. Int J Solids Struct 47:2982–2990.

Dehnhardt G, Mauck B, Hyvärinen H. 1998. Ambient temperature does not affect the tactile sensitivity of mystacial vibrissae in harbour seals. J Exp Biol 201:3023–3029.

Dörfl J. 1982. The musculature of the mystacial vibrissae of the white mouse. J Anat 135:147–154.

Geerlings M, Peters GWM, Ackermans PAJ, Oomens CWJ, Baaijens FPT. 2008. Linear viscoelastic behavior of subcutaneous adipose tissue. Biorheology 45:677–688.

Georgakoudi I, Jacobson BC, Muller MG, Sheets EE, Badizadegan K, Carr-Locke D, Crum CP, Boone CW, Dasari RR, Van Dam J, Feld MS. 2002. NAD(P)H and collagen as *in vivo* quantitative fluorescent biomarkers of epithelial precancerous changes. Cancer Res 62:682–687.

Grant RA, Mitchinson B, Fox CW, Prescott TJ. 2009. Active touch sensing in the rat: anticipatory and regulatory control of whisker movements during surface exploration. J Neurophysiol 101:862–874.

Haidarliu S, Ahissar E. 2001. Size gradients of barreloids in the rat thalamus. J Comp Neurol 429:372–387.

Haidarliu S, Simony E, Golomb D, Ahissar E. 2010. Muscle architecture in the mystacial pad of the rat. Anat Rec 293:1192–1206.

Hausman GJ, Campion DR, Richardson RL, Martin RJ. 1981. Adipocyte development in the rat hypodermis. Am J Anat 161:85–100.

Hill DN, Bermejo R, Zeigler HP, Kleinfeld D. 2008. Biomechanics of the vibrissa motor plant in rat: rhythmic whisking consists of triphasic neuromuscular activity. J Neurosci 28:3438–3455.

Icardo JM, Colvee E. 1998. Collagenous skeleton of the human mitral papillary muscle. Anat Rec 252:509–518.

Jahoda CAB, Whitehouse CJ, Reynolds AJ, Hole N. 2003. Hair follicle dermal cells differentiate into adipogenic and osteogenic lineages. Exp Dermatol 12:849–959.

Jamdar SC, Osborne LJ, Wells GN. 1986. Glycerolipid biosynthesis in rat adipose tissue. Influence of age and cell size on substrate utilization. Lipids 21:460–464.

Jamdar SC, Osborne LJ, Zeigler JA. 1981. Glycerolipid biosynthesis in rat adipose tissue. Influence of adipocyte size. Biochem J 194: 293–298.

Johanson WG, Pierce AK. 1972. Effects of elastase, collagenase, and papain on structure and function of rat lungs *in vitro*. J Clin Invest 51:288–293.

Kawamata S, Ozawa J, Hashimoto M, Kurose T, Shinohara H. 2003. Structure of the rat subcutaneous connective tissue in relation to its sliding mechanism. Arch Histol Cytol 66:273–279.

Knutsen PM, Biess A, Ahissar E. 2008. Vibrissal kinematics in 3D: tight coupling of azimuth, elevation, and torsion across different whisking modes. Neuron 59:35–42.

Kollias N, Gillies R, Moran M, Kochevar IE, Anderson RR. 1998. Endogenous skin fluorescence includes bands that may serve as quantitative marker for aging and photoaging. J Invest Dermatol 111:776–780.

Lanir Y. 1979. A structural theory for the homogenous biaxial stress-strain relationships in flat collagenous tissues. J Biomech 12:423–436.

Lübke J. 1993. Photoconversion of diaminobenzidine with different fluorescent neuronal markers into a light and electron microscopic dense reaction product. Microsc Res Tech 24:2–14.

Mariman ECM, Wang P. 2010. Adipocyte extracellular matrix composition, dynamics and role in obesity. Cell Mol Life Sci 67:1277–1292.

Melaragno HP, Montagna W. 1953. The tactile hair follicles of the mouse. Anat Rec 115:129–149.

Motta P. 1975. Scanning electron microscopic observations of mammalian adipose cells. J Microsc 22:15–20.

Na R, Stender IM, Henriksen M, Wulf HC. 2001. Autofluorescence of human skin is age-related after correction for skin pigmentation and redness. J Invest Dermatol 116:536–540.

Odetti PR, Borgoglio A, Rolandi R. 1992. Age-related increase of collagen fluorescence in human subcutaneous tissue. Metabolism 41:655–658.

Ottani V, Raspanti M, Ruggeri A. 2001. Collagen structure and functional implications. Micron 32:251–260.

Perez-Tamayo R, Montfort I. 1980. The susceptibility of hepatic collagen to homologous collagenase in human and experimental cirrhosis of the liver. Am J Pathol 100:427–440.

Pope AJ, Sands GB, Smaill BH, LeGrice IJ. 2008. Three-dimensional transmural organization of perimysial collagen in the heart. Am J Physiol Heart Circ Physiol 295:H1243–H1252.

Reith A, Schüler B. 1972. Demonstration of cytochrome oxidase activity with diaminobenzidine. A biochemical and electron microscopic study. J Histochem Cytochem 20:583–589.

Rice FL. 1993. Structure, vascularization, and innervation of the mystacial pad of the rat as revealed by the lectin *Griffonia simplicifolia*. J Comp Neurol 337:386–399.

Rothstein EC, Carroll S, Combs CA, Jobsis PD, Balaban RS. 2005. Skeletal muscle NAD(P)H two-photon fluorescence microscopy *in vivo*: topology and optical inner filters. Biophys J 88:2165–2176.

Sakita S, Ohtani O, Morohashi M. 1994. The three-dimensional microvascular and collagen fibrillar arrangements around rat vibrissa hairs as revealed by scanning electron microscopy. Med Electron Microsc 27:80–86.

Seligman AM, Karnovsky MJ, Wasserkrug HL, Hanker JS. 1968. Nondroplet ultrastructural demonstration of cytochrome oxidase activity with a polymerizing osmophilic reagent, diaminobenzidine (DAB). J Cell Biol 38:1–14.

Shi L, Ermis R, Garcia A, Telgenhoff D, Aust D. 2010. Degradation of human collagen isoforms by *Clostridium* collagenase and the effects of degradation products on cell migration. Int Wound J 7:87–95.

Simony E, Bagdasarian K, Herfst L, Brecht M, Ahissar E, Golomb D. 2010. Temporal and spatial characteristics of vibrissa responses to motor commands. J Neurosci 30:8935–8952.

Skala MC, Squirrell JM, Vrotsos KM, Eickhoff JC, Gendron-Fitzpatrick A, Eliceiri KW, Ramanujam N. 2005. Multiphoton microscopy of endogenous fluorescence differentiates normal, precancerous, and cancerous squamous epithelial tissues. Cancer Res 65:1180–1186.

Swatland HJ. 1987. Autofluorescence of adipose tissue measured with fiber optics. Meat Sci 19:277–284.

Ushiki T. 2002. Collagen fibers, reticular fibers and elastic fibers. A comprehensive understanding from a morphological viewpoint. Arch Histol Cytol 65:109–126.

Vincent SB. 1913. The tactile hair of the white rat. J Comp Neurol 23:1–36.

Wiberg C, Heinegard D, Wenglen C, Timpl B, Morgelin M. 2002. Biglykan organizes collagen VI into hexagonal-like networks resembling tissue structures. J Biol Chem 277:49120–49126.

Wineski LE. 1985. Facial morphology and vibrissal movement in the golden hamster. J Morphol 183:199–217.

Wyatt KEK, Bourne JW, Torzilli PA. 2009. Deformation-dependent enzyme mechanokinetic cleavage of type I collagen. J Biomech Eng 131:051004.

Yamada K, Semba R, Ding XH, Ma N, Nagahama M. 2005. Discrimination of cell nuclei in early S-phase, mid-to-late S-phase, and G2/M-phase by sequential administration of 5-bromo-2'-deoxiuridine and 5-chloro-2'-deoxyuridine. J Histochem Cytochem 53: 1365–1370.